SIAM J. NUMER. ANAL.
Vol. 58, No. 1, pp. 234–253

TWO-LEVEL GALERKIN MIXED FINITE ELEMENT METHOD FOR DARCY–FORCHHEIMER MODEL IN POROUS MEDIA*

FAISAL A. FAIRAG† AND JOHNSON D. AUDU†

Abstract. A two-level mixed finite element method is developed and analyzed to solve the Darcy–Forchheimer equation modeling non-Darcy flows in porous media. Instead of solving a large nonlinear system of equations on a fine mesh, the two-level method provides the flexibility of solving a small nonlinear system of equations on a coarse mesh with mesh size H followed by solving one linear system of equations on a fine mesh with mesh size h. In constructing the two-level algorithm, we introduce a small positive constant ϵ to the original nonlinear term of the Darcy–Forchheimer equation to avoid difficulties associated with nondifferentiability of the Euclidean norm at zero. The priori error estimates for the velocity and pressure gradient are obtained in L^2 and $L^{3/2}$ discrete norms, respectively. These estimates state that if piecewise constant velocities and piecewise continuous, linear pressures are used, then the coarse and fine meshes are related by $h = O(H^2)$. Numerical examples are provided to show the efficiency and accuracy of the method. Numerical results show that the two-level Galerkin mixed finite element method is computationally more cost-effective than the standard Galerkin mixed finite element and the rate of convergence also agrees with the theoretical results.

Key words. two-level method, Darcy–Forchheimer model, porous media, mixed finite element

AMS subject classifications. 76S05, 65N12, 65N15, 65N30

DOI. 10.1137/17M1158161

1. Introduction.

Let $\Omega \subset \mathbb{R}^2$ be an open bounded subset with Lipschitz boundary $\partial\Omega$. Consider a steady Darcy–Forchheimer equation, describing a single phase flow of fluid through a porous medium Ω,

$$\frac{\mu}{\rho}\boldsymbol{K}^{-1}\boldsymbol{u} + \frac{\beta}{\rho}|\boldsymbol{u}|\boldsymbol{u} + \bigtriangledown p = \boldsymbol{f} \qquad \text{in} \qquad \Omega, \tag{1}$$

$$\text{div}\boldsymbol{u} = b \qquad \text{in} \qquad \Omega, \tag{2}$$

$$\boldsymbol{u}\cdot\boldsymbol{n} = g \qquad \text{on} \qquad \partial\Omega, \tag{3}$$

where $\boldsymbol{u}$ and p denote the unknown velocity vector and pressure field, respectively. $\boldsymbol{K}$ is the permeability tensor, assumed to be bounded and uniformly positive definite. The positive parameters ρ, μ, β represent the density, viscosity, and dynamic viscosity of the fluid, respectively. $|\cdot|$ denotes the Euclidean vector norm $|\boldsymbol{u}|^2 = \boldsymbol{u}\cdot\boldsymbol{u}$, while b and g are given functions satisfying the compatibility condition,

$$\int_\Omega b(x)dx = \int_{\partial\Omega} g(\sigma)d\sigma. \tag{4}$$

The problem (1)–(4) is nonlinear and of monotone type. The existence, uniqueness, and stability of the solution is proved by Girault and Wheeler in [16]. Mixed finite element discretization of the Darcy–Forchheimer equation has been accomplished by many authors. Park in [32] investigated the semidiscrete mixed finite element for the

*Received by the editors November 22, 2017; accepted for publication (in revised form) October 23, 2019; published electronically January 9, 2020.
https://doi.org/10.1137/17M1158161
†Mathematics and Statistics Department, King Fahd University of Petroleum and Minerals, 31261 Dhahran, Saudi Arabia (ffairag@kfupm.edu.sa, http://faculty.kfupm.edu.sa/math/ffairag/, Johnson.audu@kfupm.edu.sa).

Forchheimer equation. Girault and Wheeler in [16] discretized the velocity vector and pressure with piecewise constants and Crouziex–Raviart elements, respectively. Pan and Rui in [31] approximated the velocity and pressure by mixed element such as Raviart–Thomas and Brezzi–Douglas–Marini elements. A comparison between different numerical discretizations of the Darcy–Forchheimer equation is considered in [28]. Rui and Pan in [34, 35] proposed the block-centered finite difference method, and Rui, Zhao, and Pan in [36] presented a block-centered finite difference method with variable nonlinear parameter. Wang and Rui in [39] constructed a stabilized method using the Crouzeix–Raviart element. However, irrespective of the method of discretization, the Darcy–Forchheimer equation gives rise to a system of nonlinear equation which is computationally expensive. The alternating direction iterative method of Peaceman–Rashford type was utilized in [16] to solve the resulting nonlinear system, and Newton's iterative method was used in [28]. Huang, Chen, and Rui in [21] applied a full approximation scheme to construct a V-cycle multigrid method for the nonlinear Darcy–Forchheimer equation.

The two-level method was introduced by Xu [40, 41] in his quest to reduce the computational cost of nonlinear systems of equations. The method starts by solving one small, nonlinear system of equations on a coarse mesh $\mathcal{T}_H$ with mesh size H to obtain a rough approximation followed by solving large linear system of equations on a finer mesh $\mathcal{T}_h$ of size h with $h << H$ to produce a corrected solution. Many authors have since explored this technique for different nonlinear equations, for instance, Layton [23], Layton and Lenferink [25, 24], Layton and Tobiska [26], Fairag [11, 12, 13], Foster, Iliescu, and Wells [14], Dawson and Wheeler [9], Dawson, Wheeler, and Woodward [10], Chen, Liu, and Liu [7], He [18, 17], He and Li [19], and Li and Rui [27].

The first attempt to solve the Darcy–Forcheimer model using a two-level method was accomplished by Rui and Liu in [33]. They obtained approximate solution using a two-grid block-centered finite difference method. In addition, error estimates of order $O(h^2 + H^4 + \epsilon)$ were obtained, for both velocity and pressure, and ϵ is a small positive parameter. To the best of our knowledge, no research work has incorporated the two-level method with mixed finite element to solve the Darcy–Forchheimer model.

The main purpose of this paper is to develop and implement a two-level mixed finite element discretization of the nonlinear Darcy–Forchheimer model in two dimensions. The nonlinear term of the Darcy–Forchheimer equation contains the Euclidean norm of the velocity $|\boldsymbol{u}|$ which is not differentiable at zero. Therefore, to construct the two-level algorithm, we smoothen the nonlinear term by introducing a small positive parameter ϵ as in [33]. In this paper, we prove that the error estimates of the two-level mixed finite element method are of order $O(\epsilon h + h + H^2 + \epsilon)$ for velocity and gradient pressure in L^2 and $L^{\frac{3}{2}}$ discrete norms, respectively, H is the coarse mesh size, and h is the fine mesh size. Some numerical experiments are carried out to investigate the effectiveness and accuracy of the method. Compared to the standard mixed finite element method in [37, 28], the two-level mixed element algorithm provides the same accuracy with less computational time.

The materials in this paper are arranged as follows. Section 2 contains some preliminaries needed for this work, section 3 states the variational formulation, and section 4 covers the approximation spaces and discretization. In section 5 we present the two-level algorithm and its well-posedness. Error estimates are presented in section 6, and section 7 discusses the solutions of the systems of equations resulting from the two-level algorithm in section 5. Numerical results are displayed in section 8.

2. Preliminaries. In this section, we present some fundamental notations, definitions, and theorems used in this study.

Let $\alpha = (\alpha_1, \alpha_2, \alpha_3, \ldots, \alpha_d)$, $\alpha_i \in \mathbb{N}$, be multi-index with $|\alpha| = \alpha_1 + \alpha_2 + \alpha_3 + \cdots + \alpha_d$.
Define the partial derivatives,

$$\mathcal{D}^\alpha = \frac{\partial^{|\alpha|}}{\partial x_1^{\alpha_1} \partial x_2^{\alpha_2} \partial x_3^{\alpha_3} \cdots \partial x_d^{\alpha_d}} \quad .$$

For any $m \in N$ and $1 \leq p \leq +\infty$, we define the Sobolev space (see [2]),

$$W^{m,p} = \{u \in L^p : \mathcal{D}^\alpha u \in L^p(\Omega), |\alpha| \leq m\},$$

equipped with the norm,

$$\|u\|_{W^{m,p}} = \|u\|_{L^p(\Omega)} + \sum_{0<|\alpha\| \leq m} \|\mathcal{D}^\alpha u\|_{L^p(\Omega)}.$$

For $p = 2$, $W^{m,p}(\Omega) = H^m(\Omega)$ is a Hilbert space. Extension of these definitions to vectors and tensors can be done with some modification for the norms. Considering a vector or a tensor $\boldsymbol{u}$, we denote

$$\|\boldsymbol{u}\|_{L^p(\Omega)} = \left(\int_\Omega |\boldsymbol{u}(\boldsymbol{x})|^p d\boldsymbol{x} \right)^{\frac{1}{p}} ,$$

where $|\cdot|$ denotes the Euclidean norm.

3. Functional settings and weak formulation. In order to write (1)–(4) in variational form, we define the following spaces:

$$\begin{aligned} L_0^2(\Omega) &= \left\{ \boldsymbol{v} : \boldsymbol{v} \in L^2(\Omega), \int_\Omega \boldsymbol{v}(x) dx = 0 \right\}, \\ X &= L^3(\Omega)^2, \\ M &= W^{1,3/2}(\Omega) \cap L_0^2(\Omega). \end{aligned}$$

Assume that $b \in L^{6/5}(\Omega)$ and $g \in L^{3/2}(\partial\Omega)$; we then consider the weak formulation: Find $(\boldsymbol{u}, p) \in X \times M$ such that

$$\frac{\mu}{\rho} \int_\Omega (K^{-1}\boldsymbol{u}) \cdot \boldsymbol{\varphi} dx + \frac{\beta}{\rho} \int_\Omega |\boldsymbol{u}|\boldsymbol{u} \cdot \boldsymbol{\varphi} d\boldsymbol{x} + \int_\Omega \nabla p \cdot \boldsymbol{\varphi} d\boldsymbol{x} = \int_\Omega \boldsymbol{f} \cdot \boldsymbol{\varphi} d\boldsymbol{x} \quad \forall \varphi \in X, \tag{5}$$

$$\int_\Omega \nabla q \cdot \boldsymbol{u} d\boldsymbol{x} = -\int_\Omega bq\boldsymbol{d}x + \int_{\partial\Omega} gq\boldsymbol{d}\sigma \ \forall q \in M. \tag{6}$$

Setting

$$\begin{aligned} a(\boldsymbol{u}, \boldsymbol{\varphi}) &= \frac{\mu}{\rho} \int_\Omega (K^{-1}\boldsymbol{u}) \cdot \boldsymbol{\varphi} dx + \frac{\beta}{\rho} \int_\Omega |\boldsymbol{u}|\boldsymbol{u} \cdot \boldsymbol{\varphi} d\boldsymbol{x} \ , \\ b(\boldsymbol{u}, q) &= \int_\Omega \nabla q \cdot \boldsymbol{u} d\boldsymbol{x} \ , \end{aligned}$$

the variational formulation (5)–(6) takes the form of a saddle point problem [5, 6]. The equivalence of (5)–(6) to the original problem (1)–(3) follows by the virtue of the Green's formula,

$$\int_{\Omega} \boldsymbol{v} \cdot \bigtriangledown q dx = -\int_{\Omega} \operatorname{div} \boldsymbol{v} dx + \langle q,\ \boldsymbol{v}.n\rangle_{\partial\Omega} \quad \forall q \in M,\ \forall \boldsymbol{v} \in H, \tag{7}$$

where

$$H = \left\{ \boldsymbol{v} \in L^3(\Omega) : \operatorname{div}\boldsymbol{v} \in L^{6/5}(\Omega) \right\}.$$

Let

$$V = \left\{ \boldsymbol{v} \in X; \int_{\Omega} \bigtriangledown q \cdot u d\boldsymbol{x} = 0\ \forall\ q \in M \right\}.$$

For $d = 2$ or 3, it is shown in [16] that for $b \in L^{3d/2+3}(\Omega)$ and $g \in L^{3(d-1)/d}(\partial\Omega)$ there is a unique $\boldsymbol{u}_\ell \in L^3(\Omega)^d/V$ satisfying the following:

$$\int_{\Omega} \bigtriangledown q \cdot \boldsymbol{u}_\ell d\boldsymbol{x} = -\int_{\Omega} bq\boldsymbol{d}x + \int_{\partial\Omega} gq\boldsymbol{d}\sigma \quad \forall q \in M, \tag{8}$$

$$\|\boldsymbol{u}_\ell\|_{L^3(\Omega)^d/V} \le C \left(\|b\|_{L^{\frac{3d}{d+3}}(\Omega)} + \|g\|_{L^{\frac{3(d-1)}{d}}} \right), \tag{9}$$

where C depends on Ω and d.

The nonlinear map associated with $a(\boldsymbol{u}, \phi)$ given by the mapping $\boldsymbol{v} \mapsto \mathcal{A}(\boldsymbol{v})$ is defined by

$$\forall \boldsymbol{v} \in L^3(\Omega)^d, \mathcal{A}(\boldsymbol{v}) = \frac{\mu}{\rho} K^{-1}\boldsymbol{v} + \frac{\beta}{\rho}|\boldsymbol{v}|\boldsymbol{v}. \tag{10}$$

Assuming $\lambda_{min} > 0$ is the minimum eigenvalue of K, it was demonstrated in [16] that the nonlinear map $\mathcal{A}$ is bounded, monotone, coercive, and hemicontinuous. Furthermore, the bilinear form

$$b(\boldsymbol{v}, q) = \int_{\Omega} \bigtriangledown q \cdot \boldsymbol{v} d\boldsymbol{x}$$

satisfies the following infsup condition:

$$\inf_{0 \ne q \in M} \sup_{0 \ne v \in X} \frac{b(\boldsymbol{v}, q)}{\|\boldsymbol{v}\|_{L^3(\Omega)} \| \bigtriangledown q\|_{L^{\frac{3}{2}}(\Omega)}} = 1. \tag{11}$$

With these properties of $\mathcal{A}$ and the infsup condition in (11), Girault and Wheeler in [16] established the well-posedness of (5)–(6). The following prior estimates hold for all liftings $\boldsymbol{u}_{\boldsymbol{\ell}}$ in $L^3(\Omega)^d$:

$$\|\boldsymbol{u}\|_{L^3(\Omega)} \le \left(\|\boldsymbol{u}_{\boldsymbol{\ell}}\|_{L^3(\Omega)} + \frac{3}{4}\frac{\mu}{\rho}\frac{\|K^{-1}\|_{L^\infty(\Omega)}}{\lambda_{min}} \|\boldsymbol{u}_{\boldsymbol{\ell}}{}^2_{L^2(\Omega)} \right)^{\frac{1}{3}}, \tag{12}$$

$$\| \bigtriangledown p\|_{L^{\frac{3}{2}}(\Omega)} \le \frac{\mu}{\rho}\|K^{-1}\|_{L^\infty(\Omega)} \|\boldsymbol{u}\|_{L^{\frac{3}{2}}(\Omega)} + \frac{\beta}{\rho}\|\boldsymbol{u}\|^2_{L^3(\Omega)}. \tag{13}$$

4. Discretization. Let Ω be a polygon ($d = 2$) or a Lipschitz polyhedron ($d = 3$). We assume $\mathcal{T}_h$ is a family of conforming triangulations of $\bar{\Omega}$. In addition, assume there exists a positive constant α independent of h and $T \in \mathcal{T}_h$ [8] such that

$$\forall T \in \mathcal{T}_h,\ \frac{h_T}{\rho_T} \leq \alpha, \tag{14}$$

where, h_T represents the diameter of T and ρ_T represents the diameter of the sphere inscribed in T. We discretize the velocity $\boldsymbol{u}$ and pressure p respectively in the following spaces:

$$\begin{aligned} X_h &= \left\{\boldsymbol{v} \in [L^2(\Omega)]^2; \boldsymbol{v}|T \in \mathbb{P}_0 \ \ \forall\, T \in \mathcal{T}_h, \right\}, \\ Q_h &= \left\{q \in C^0(\bar{\Omega}); q|T \in \mathbb{P}_1 \ \ \forall\, T \in \mathcal{T}_h \right\}, \\ M_h &= Q_h \cap L_0^2(\Omega). \end{aligned} \tag{15}$$

The discrete variational formulation of (5)–(6) is as follows: for all $(\boldsymbol{\varphi}_h, q_h) \in X_h \times M_h$, find $(u_h, p_h) \in X_h \times M_h$ such that

$$\frac{\mu}{\rho}\int_\Omega (K^{-1}\boldsymbol{u}_h)\cdot\boldsymbol{\varphi}_h d\boldsymbol{x} + \frac{\beta}{\rho}\int_\Omega |\boldsymbol{u_h}|\boldsymbol{u}_h\cdot\boldsymbol{\varphi}_h d\boldsymbol{x} + \int_\Omega \bigtriangledown p_h\cdot\boldsymbol{\varphi}_h d\boldsymbol{x} = \int_\Omega \boldsymbol{f}\cdot\boldsymbol{\varphi} d\boldsymbol{x}, \tag{16}$$

$$\int_\Omega \bigtriangledown q_h\cdot\boldsymbol{u}_h d\boldsymbol{x} = -\int_\Omega b q_h \boldsymbol{d}x + \int_{\partial\Omega} g q_h \boldsymbol{d\sigma}. \tag{17}$$

5. Two-level mixed finite element method. In this section, we present the two-level mixed finite element method for obtaining an approximate solution to (1)–(3). It is worthy of note that the Euclidean norm $|\boldsymbol{u}|$ is not differentiable at zero. Therefore, let

$$|\boldsymbol{u}|_\epsilon = \sqrt{|\boldsymbol{u}|^2 + \epsilon^2},$$

where ϵ is a small positive constant. For ϵ very small, it is shown in [34] that $|\boldsymbol{u}|_\epsilon$ is a good approximation for $|\boldsymbol{u}|$ and the partial derivatives of $|\boldsymbol{u}|_\epsilon$ approximate the partial derivatives of $|\boldsymbol{u}|$ very well. Particularly, $|\boldsymbol{u}|_\epsilon - |\boldsymbol{u}| < \epsilon$. Now consider the map $\boldsymbol{f}_\epsilon : \mathbb{R}^2 \longrightarrow \mathbb{R}^2$ defined by

$$\boldsymbol{f}_\epsilon(\boldsymbol{u}) = |\boldsymbol{u}|_\epsilon \boldsymbol{u}\ ,$$

$$\boldsymbol{f}_\epsilon(\boldsymbol{u}) = \begin{bmatrix}\boldsymbol{f}_{\epsilon,1}(\boldsymbol{u})\\ \boldsymbol{f}_{\epsilon,2}(\boldsymbol{u})\end{bmatrix} = \begin{bmatrix}|\boldsymbol{u}|_\epsilon u_1\\ |\boldsymbol{u}|_\epsilon u_2\end{bmatrix}\ .$$

The Taylor series representation of $\boldsymbol{f}_\epsilon(\boldsymbol{u})$ about $\boldsymbol{u}_H \in \mathbb{R}^2$ is given by

$$\boldsymbol{f}_\epsilon(\boldsymbol{u}) = \boldsymbol{f}_\epsilon(\boldsymbol{u}_H) + \mathcal{D}\boldsymbol{f}_\epsilon(\boldsymbol{u}_H)(\boldsymbol{u}-\boldsymbol{u}_H) + \frac{1}{2!}\mathcal{D}^2\boldsymbol{f}_\epsilon(\boldsymbol{\zeta}_H)(\boldsymbol{u}-\boldsymbol{u}_H)^2\ , \tag{18}$$

where $\boldsymbol{\zeta}_H = t\ \boldsymbol{u} + (1-t)\ \boldsymbol{u}_H$ for some t in $[0,1]$ and $(\boldsymbol{u}-\boldsymbol{u}_H)^2$ is expressed as Kronecker product $(\boldsymbol{u}-\boldsymbol{u}_H)\otimes(\boldsymbol{u}-\boldsymbol{u}_H)$. Precisely, $(\boldsymbol{u}-\boldsymbol{u}_H)^2$ is equal to

$$[(u_1-u_{H,1})^2, (u_1-u_{H,1})(u_2-u_{H,2}), (u_2-u_{H,2})(u_1-u_{H,1}), (u_2-u_{H,2})^2]^T.$$

$\mathcal{D}\boldsymbol{f}_\epsilon(\boldsymbol{u}_H)$ and $\mathcal{D}^2\boldsymbol{f}_\epsilon(\boldsymbol{\zeta}_H)$ are given as follows:

$$\mathcal{D}\boldsymbol{f}_\epsilon(\boldsymbol{u}_H) = \begin{pmatrix}\frac{\partial \boldsymbol{f}_{\epsilon,1}(\boldsymbol{u}_H)}{\partial u_1} & \frac{\partial \boldsymbol{f}_{\epsilon,1}(\boldsymbol{u}_H)}{\partial u_2}\\ \frac{\partial \boldsymbol{f}_{\epsilon,2}(\boldsymbol{u}_H)}{\partial u_1} & \frac{\partial \boldsymbol{f}_{\epsilon,2}(\boldsymbol{u}_H)}{\partial u_2}\end{pmatrix}\ ,$$

$$\mathcal{D}^2\boldsymbol{f}_\epsilon(\boldsymbol{\zeta}_H) = \begin{pmatrix}\frac{\partial^2 \boldsymbol{f}_{\epsilon,1}(\boldsymbol{\zeta}_H)}{\partial u_1^2} & \frac{\partial^2 \boldsymbol{f}_{\epsilon,1}(\boldsymbol{\zeta}_H)}{\partial u_1\partial u_2} & \frac{\partial^2 \boldsymbol{f}_{\epsilon,1}(\boldsymbol{\zeta}_H)}{\partial u_2\partial u_1} & \frac{\partial^2 \boldsymbol{f}_{\epsilon,1}(\boldsymbol{\zeta}_H)}{\partial u_2^2}\\ \frac{\partial^2 \boldsymbol{f}_{\epsilon,2}(\boldsymbol{\zeta}_H)}{\partial u_1^2} & \frac{\partial^2 \boldsymbol{f}_{\epsilon,2}(\boldsymbol{\zeta}_H)}{\partial u_1\partial u_2} & \frac{\partial^2 \boldsymbol{f}_{\epsilon,2}(\boldsymbol{\zeta}_H)}{\partial u_2\partial u_1} & \frac{\partial^2 \boldsymbol{f}_{\epsilon,2}(\boldsymbol{\zeta}_H)}{\partial u_2^2}\end{pmatrix}\ .$$

In view of (18), for any $\boldsymbol{\varphi} = (\varphi_1, \varphi_2) \in \mathbb{R}^2$,

$$\boldsymbol{f}_\epsilon(\boldsymbol{u}) \cdot \boldsymbol{\varphi} = \sum_{i=1}^{2} \boldsymbol{f}_{\epsilon,i}(\boldsymbol{u}_H)\varphi_i + \sum_{i=1}^{2}\sum_{j=1}^{2} \frac{\partial \boldsymbol{f}_{\epsilon,i}(\boldsymbol{u}_H)}{\partial u_j}(u_j - u_{H,j})\varphi_i$$

$$+ \sum_{k=1}^{2}\sum_{j=1}^{2}\sum_{i=1}^{2} \frac{\partial^2 \boldsymbol{f}_{\epsilon,k}(\boldsymbol{\zeta}_H)}{\partial u_i \partial u_j}(u_i - u_{H,i})(u_j - u_{H,j})\varphi_k \ . \tag{19}$$

Lemma 5.1. *The first and second order partial derivatives of $\boldsymbol{f}_\epsilon$ exist, and they are bounded and continuous.*

Proof. Direct differentiation shows that

$$\frac{\partial \boldsymbol{f}_{\epsilon,i}(\boldsymbol{u})}{\partial u_j} = (u_i u_j + |\boldsymbol{u}|_\epsilon^2 \delta_{ij})|\boldsymbol{u}|_\epsilon^{-1}, \quad i, j = 1, 2 \ ,$$

$$\delta_{ij} = \begin{cases} 1, i = j, \\ 0, i \neq j. \end{cases}$$

$$\frac{\partial^2 \boldsymbol{f}_{\epsilon,k}(\boldsymbol{u})}{\partial u_i u_j} = (2u_i|\boldsymbol{u}|_\epsilon^2 \delta_{ijk} - u_i u_j u_k + u_s|\boldsymbol{u}|_\epsilon^2)|\boldsymbol{u}|_\epsilon^{-3}, \quad i, j, k = 1, 2 \ ,$$

$$\delta_{ijk} = \begin{cases} 1, & i = j = k, \\ 0 & \text{otherwise}, \end{cases} \qquad s = \begin{cases} k, & i = j = k, \\ k, & i = j \neq k, \\ j, & i \neq j, k = i, \\ i, & i \neq j, k = j. \end{cases}$$

Furthermore, there exist constants C_1, C_2 such that

$$\left|\frac{\partial \boldsymbol{f}_{\epsilon,i}(\boldsymbol{u})}{\partial u_j}\right| \leq (C_1 + \epsilon), \quad \left|\frac{\partial^2 \boldsymbol{f}_{\epsilon,k}(\boldsymbol{u})}{\partial u_i u_j}\right| \leq C_2, \quad i, j, k = 1, 2 \ . \tag{20}$$ □

We now present the two-level algorithm.

5.1. Two-level algorithm. Let $X_H, X_h \subset X, M_H, M_h \subset M$ denote finite element spaces as defined in (15) with $X_H \subset X_h, M_H \subset M_h$, $H \gg h$.

Step 1. Solve the nonlinear system on a coarse mesh $\mathcal{T}_H$ with mesh size H: For all $(\boldsymbol{\varphi}_H, q_H) \in X_H \times M_H$, find $(\boldsymbol{u}_H, p_H) \in X_H \times M_H$ such that

(21)
$$\frac{\mu}{\rho}\int_\Omega (K^{-1}\boldsymbol{u}_H) \cdot \boldsymbol{\varphi}_H d\boldsymbol{x} + \frac{\beta}{\rho}\int_\Omega |\boldsymbol{u}_{\boldsymbol{H}}|\boldsymbol{u}_H \cdot \boldsymbol{\varphi}_H d\boldsymbol{x} + \int_\Omega \triangledown p_H \cdot \boldsymbol{\varphi}_H d\boldsymbol{x} = \int_\Omega \boldsymbol{f} \cdot \boldsymbol{\varphi}_H d\boldsymbol{x},$$

(22)
$$\int_\Omega \triangledown q_H \cdot \boldsymbol{u}_{\boldsymbol{H}} d\boldsymbol{x} = -\int_\Omega b q_H \boldsymbol{d}x + \int_{\partial\Omega} g q_H \boldsymbol{d}\sigma,$$

Step 2. Solve the linear system on a fine mesh $\mathcal{T}_h$ with mesh size h: For all $(\boldsymbol{\varphi}_h, q_h) \in X_h \times M_h$, find $(\boldsymbol{u}_h, p_h) \in X_h \times M_h$ such that

$$\frac{\mu}{\rho}\int_\Omega (K^{-1}\boldsymbol{u}_h) \cdot \boldsymbol{\varphi}_h dx + \frac{\beta}{\rho}\int_\Omega \mathcal{D}\boldsymbol{f}_\epsilon(\boldsymbol{u}_H)\boldsymbol{u}_h \cdot \boldsymbol{\varphi}_h d\boldsymbol{x} + \int_\Omega \triangledown p_h \cdot \boldsymbol{\varphi}_h d\boldsymbol{x}$$

$$= \int_\Omega \boldsymbol{f}\boldsymbol{\varphi}_h dx - \frac{\beta}{\rho}\int_\Omega |\boldsymbol{u}_{\boldsymbol{H}}|_{\boldsymbol{\epsilon}}\boldsymbol{u}_{\boldsymbol{H}} \cdot \boldsymbol{\varphi}_h d\boldsymbol{x} + \frac{\beta}{\rho}\int_\Omega \mathcal{D}\boldsymbol{f}_\epsilon(\boldsymbol{u}_H)\boldsymbol{u}_H \cdot \boldsymbol{\varphi}_h d\boldsymbol{x}, \tag{23}$$

$$\int_\Omega \triangledown q_h \cdot \boldsymbol{u}_h d\boldsymbol{x} = -\int_\Omega b q_h \boldsymbol{d}x + \int_{\partial\Omega} g q_h \boldsymbol{d}\sigma. \tag{24}$$

The well-posedness of this algorithm will be presented in the next section.

5.2. Well-posedness of the discrete problem in Step 2. The well-posedness of (21)–(22) is well established in [16]. We now discuss the well-posedness of (23)–(24).

5.2.1. Existence and uniqueness. Let V_h represent the discrete analogue of V.

$$V_h = \left\{ \boldsymbol{v}_h \in X_h; \sum_{T \in \mathcal{T}_h} \int_T \triangledown q_h \cdot \boldsymbol{v}_h d\boldsymbol{x} = 0 \quad \forall q_h \in M_h \right\}.$$

Define

$$\bar{a} : V_h \times V_h \longrightarrow \mathbb{R}, \quad \bar{b} : M_h \times X_h \longrightarrow \mathbb{R},$$

with

$$\bar{a}(\boldsymbol{u}_h, \boldsymbol{\varphi_h}) = \frac{\mu}{\rho} \int_\Omega (K^{-1}\boldsymbol{u}_h) \cdot \boldsymbol{\varphi}_h dx + \frac{\beta}{\rho} \int_\Omega \mathcal{D}\boldsymbol{f}_\epsilon(\boldsymbol{u}_H)\boldsymbol{u}_h \cdot \boldsymbol{\varphi}_h d\boldsymbol{x} \ , \tag{25}$$

$$\bar{b}(q_h, \boldsymbol{u_h}) = \int_\Omega \triangledown q_h \boldsymbol{u}_h d\boldsymbol{x} \ . \tag{26}$$

where $\bar{a}$ as defined in (25) is bilinear. Then problem (23)–(24) becomes, for all $\boldsymbol{\varphi_h} \in V_h$, to find $\boldsymbol{u_h} \in V_h$ such that

$$\bar{a}(\boldsymbol{u_h}, \boldsymbol{\varphi_h}) = \int_\Omega \boldsymbol{f} \cdot \boldsymbol{\varphi}_h d\boldsymbol{x} - \frac{\beta}{\rho} \int_\Omega |\boldsymbol{u_H}|_{\boldsymbol{\epsilon}} \boldsymbol{u_H} \cdot \boldsymbol{\varphi}_h d\boldsymbol{x} + \int_\Omega \frac{\beta}{\rho} \mathcal{D}\boldsymbol{f}_\epsilon(\boldsymbol{u}_H)\boldsymbol{u}_H \cdot \boldsymbol{\varphi}_h d\boldsymbol{x}. \tag{27}$$

LEMMA 5.2. *The bilinear form $\bar{a}$ is V_h-elliptic and the bilinear form $\bar{b}$ satisfies the following discrete* "infsup" *condition:*

(28)

$$\forall q_h \in M_h \sup_{u_h \in X_h} \left(\frac{1}{\|u_h\|_{L^3(\Omega)}} \sum_{T \in \mathcal{T}_h} \int_T \triangledown q_h \cdot \boldsymbol{u}_h d\boldsymbol{x} \right) = \left(\sum_{T \in \mathcal{T}_h} \| \triangledown q_h \|^{3/2}_{L^{3/2}(T)} \right)^{2/3} .$$

Proof.

$$\begin{aligned} \bar{a}(\boldsymbol{u_h}, \boldsymbol{u_h}) &= \frac{\mu}{\rho} \int_\Omega (K^{-1}\boldsymbol{u}_h) \cdot \boldsymbol{u}_h dx + \frac{\beta}{\rho} \int_\Omega \mathcal{D}\boldsymbol{f}_\epsilon(\boldsymbol{u}_H)\boldsymbol{u}_h \cdot \boldsymbol{u}_h d\boldsymbol{x} \\ &\geq \frac{\mu}{\rho} \lambda_{min} \|u_h\|^2_{L^2(\Omega)} + \frac{\beta}{\rho} \min_{i,j=1,2} \left| \frac{\partial \boldsymbol{f}_{\epsilon,i}(\boldsymbol{u}_H)}{\partial u_j} \right| \|\boldsymbol{u_h}\|^2_{L^2(\Omega)}, \end{aligned}$$

$$\bar{a}(\boldsymbol{u_h}, \boldsymbol{u_h}) \geq \frac{\mu}{\rho} \lambda_{min} \|\boldsymbol{u_h}\|^2_{L^2(\Omega)} \quad \forall \boldsymbol{u_h} \in V_h. \tag{29}$$

For the infsup condition in 28 (see Proposition 4.1 in [37]). Thanks to Lemma 5.2, extension of the Babuška–Brezzi theory to reflexive Banach space [3, 6, 20] guarantees the existence and uniqueness of the solution of (23)–(24). □

5.2.2. Stability. Theorem 3 in [16] established the stability of (21)–(22), particularly for any data $(b, g) \in L^{\frac{6}{5}}(\Omega) \times L^{\frac{3}{2}}(\partial\Omega)$ satisfying (4) and $\boldsymbol{u}_{H_\ell} \in X_H$ satisfying (22). The unique solution $(\boldsymbol{u}_H, p_H) \in X_H \times M_H$ of (21)–(22) satisfies the following bounds:

$$\|\boldsymbol{u}_H\|_{L^3(\Omega)} \leq \left(\|\boldsymbol{u}_{H_\ell}\|_{L^3(\Omega)} + \frac{3}{4} \frac{\mu}{\rho} \frac{\|K^{-1}\|_{L^\infty(\Omega)}}{\lambda_{min}} \|\boldsymbol{u}_{H_\ell}\|^2_{L^2(\Omega)} \right)^{\frac{1}{3}}, \tag{30}$$

where $\boldsymbol{u}_{H_\ell}$ satisfies the discrete analogue of (9),

$$\| \triangledown p_H \|_{L^{\frac{3}{2}}(\Omega)} \leq \frac{\mu}{\rho} \|K^{-1}\|_{L^\infty(\Omega)} \|\boldsymbol{u}\|_{L^{\frac{3}{2}}(\Omega)} + \frac{\beta}{\rho} \|\boldsymbol{u}\|^2_{L^3(\Omega)}. \tag{31}$$

Now we present the stability of (23)–(24).

THEOREM 5.3. *Let $(\boldsymbol{u_H}, p_H) \in X_H \times M_H$ be the unique solution of* (21)–(22) *and $(\boldsymbol{u_h}, P_h) \in X_h \times M_h$ be the unique solution of* (23)–(24)*; then for each $(b, g) \in L^{\frac{6}{5}}(\Omega) \times L^{\frac{3}{2}}(\partial\Omega)$ satisfying* (4)*, the following bounds hold:*

$$\|u_h\|_{L^2(\Omega)} \leq \frac{\rho}{\mu\lambda_{min}}\|\boldsymbol{f}\|_{L^2(\Omega)} + \frac{\beta}{\mu\lambda_{min}}(C+\epsilon)\left(\|\boldsymbol{u}_{H_\ell}\|_{L^3(\Omega)} + \frac{3}{4}\frac{\mu}{\rho}\frac{\|K^{-1}\|_{L^\infty(\Omega)}}{\lambda_{min}}\|\boldsymbol{u}_{H_\ell}\|^2_{L^2(\Omega)}\right)^{\frac{1}{3}}, \tag{32}$$

$$\|\bigtriangledown p_h\|_{L^{\frac{3}{2}}(\Omega)} \leq \|\boldsymbol{f}\|_{L^{\frac{3}{2}}(\Omega)} + \left(\frac{\mu}{\rho}\|K^{-1}\|_{L^\infty(\Omega)} + \frac{\beta}{\rho}(C_1+\epsilon)\right)\|\boldsymbol{u}_h\|_{L^{\frac{3}{2}}(\Omega)} + \frac{\beta}{\rho}\left(\|\boldsymbol{u}_{H_\ell}\|_{L^3(\Omega)} + \frac{3}{4}\frac{\mu}{\rho}\frac{\|K^{-1}\|_{L^\infty(\Omega)}}{\lambda_{min}}\|\boldsymbol{u}_{H_\ell}\|^2_{L^2(\Omega)}\right)^{\frac{1}{3}}, \tag{33}$$

where C, C_1 are positive constants.

Proof. Applying (29) and Lemma 5.1 in (27) gives

$$\frac{\mu\lambda_{min}}{\rho}\|\boldsymbol{u}_h\|^2_{L^2(\Omega)} \leq \|\boldsymbol{f}\|_{L^2(\Omega)}\|\boldsymbol{u}_h\|_{L^2(\Omega)} + \frac{\beta C_2}{\rho}\|\boldsymbol{u}_H\|_{L^2(\Omega)}\|\boldsymbol{u}_h\|_{L^2(\Omega)} + \frac{\beta}{\rho}(C_1+\epsilon)\|\boldsymbol{u}_H\|_{L^2(\Omega)}\|\boldsymbol{u}_h\|_{L^2(\Omega)},$$

$$\|\boldsymbol{u}_h\|_{L^2(\Omega)} \leq \frac{\rho}{\mu\lambda_{min}}\|\boldsymbol{f}\|_{L^2(\Omega)} + \frac{\beta}{\mu\lambda_{min}}(C+\epsilon)\|\boldsymbol{u}_H\|_{L^2(\Omega)}. \tag{34}$$

Applying (30) in (34) establishes (32).

Now define

$$\tilde{\mathcal{A}}(\boldsymbol{u}_h) = \frac{\mu}{\rho}(K^{-1}\boldsymbol{u}_h) + \frac{\beta}{\rho}\mathcal{D}\boldsymbol{f}_\epsilon(\boldsymbol{u}_H)\boldsymbol{u}_h - \left(\boldsymbol{f} - \frac{\beta}{\rho}|\boldsymbol{u_H}|_{\boldsymbol{\epsilon}}\boldsymbol{u_H} + \frac{\beta}{\rho}\mathcal{D}\boldsymbol{f}_\epsilon(\boldsymbol{u}_H)\boldsymbol{u}_H\right).$$

$\tilde{\mathcal{A}}(\boldsymbol{u}_h)$ maps $L^3(\Omega)$ into $L^{\frac{3}{2}}(\Omega)$. In fact,

$$\|\tilde{\mathcal{A}}(\boldsymbol{u}_h)\|_{L^{\frac{3}{2}}(\Omega)} \leq \|\boldsymbol{f}\|_{L^{\frac{3}{2}}(\Omega)} + \left(\frac{\mu}{\rho}\|K^{-1}\|_{L^\infty(\Omega)} + \frac{\beta}{\rho}(C_1+\epsilon)\right)\|\boldsymbol{u}_h\|_{L^{\frac{3}{2}}(\Omega)} + \frac{\beta}{\rho}\|\boldsymbol{u}_H\|_{L^{\frac{3}{2}}(\Omega)}. \tag{35}$$

Equation (27) implies that $\tilde{\mathcal{A}}(\boldsymbol{u}_h)$ belongs to $(V_h^\perp)$, the orthogonal space of V_h in X_h for the inner product of $L^2(\Omega)$, where

$$V_h^\perp = \left\{\boldsymbol{v}_h \in X_h, \int_\Omega \boldsymbol{v}_h \cdot \boldsymbol{\varphi}_h d\boldsymbol{x} = 0 \quad \forall \boldsymbol{\varphi}_h \in V_h\right\}.$$

Thanks to the infsup condition in Lemma 5.2 and finite dimensional variant of Babuska–Brezzi's theory [3], there exists a unique $p_h \in M_h$ such that

$$\bigtriangledown p_h = \tilde{\mathcal{A}}(\boldsymbol{u}_h).$$

Therefore,

$$\|\bigtriangledown p_h\|_{L^{\frac{3}{2}}(\Omega)} = \|\mathcal{A}(\boldsymbol{u}_h)\|_{L^{\frac{3}{2}}(\Omega)} = \sup_{\boldsymbol{\varphi_h} \in L^3(\Omega)} \frac{\int_\Omega \mathcal{A}(\boldsymbol{u}_h)\cdot\boldsymbol{\varphi_h}d\boldsymbol{x}}{\|\boldsymbol{\varphi_h}\|_{L^3(\Omega)}} \quad \forall \boldsymbol{u_h}, \boldsymbol{\varphi_h} \in X_h, \tag{36}$$

$$\left|\int_\Omega \tilde{\mathcal{A}}(\boldsymbol{u}_h)\cdot\boldsymbol{\varphi_h}d\boldsymbol{x}\right| \le \|\tilde{\mathcal{A}}(\boldsymbol{u}_h)\|_{L^{\frac{3}{2}}(\Omega)}\|\boldsymbol{\varphi_h}\|_{L^3(\Omega)}. \tag{37}$$

In view of the estimates in (35) and (37), (33) is deduced from (36). ∎

6. Error estimates. Let $\Pi_h : L^1(\Omega)^2 \longrightarrow X_h$ be local projection on Q_h defined by

$$\forall T\in\mathcal{T}_h, \forall u\in L^1(T), \Pi_h(u)|_T = \frac{1}{|T|}\int_T u(\boldsymbol{x})d\boldsymbol{x}. \tag{38}$$

Stability properties and convergence of Π_h are well presented in [15]. In fact for any $1\le r\le\infty$,

$$\forall u\in L^r(\Omega), \lim_{h\mapsto 0}\Pi_h(u) = u \ \text{ strongly in } \ L^r(\Omega), \tag{39}$$

$$\forall u\in w^{1,r}(\Omega), \|\Pi_h(u)-u\|_{L^r(\Omega)} = O(h). \tag{40}$$

Furthermore, let $I_h(p)$ be a polynomial interpolation operator [15]; from Sobolev's space approximation theory, we have the following properties:

$$\|p-I_h(p)\|_{L^p} + h\|\bigtriangledown(p-I_h(p)\|_{L^p} \le Ch^2\|p\|_{H^2(\Omega)},$$

with $C>0$, independent of h. In particular,

$$\|\bigtriangledown(p-I_h(p))\|_{L^{3/2}(\Omega)} \le Ch|p|_{2,\frac{3}{2},(\Omega)}. \tag{41}$$

The error estimates for (21)–(22) have been established in [16] and summarized in the following theorem.

THEOREM 6.1 (see [16, 37]). *Let $(\boldsymbol{u_H}, p_H)$ be the solution of (21)–(22) and $(\boldsymbol{u}, p)$ the solution of (5)–(6) $\mathcal{T}_H$ satisfying (14), and assume $\boldsymbol{u}$ belongs to $W^{1,4}(\Omega)^d$. Then we have the following error bounds:*

$$\|u-u_H\|_{L^2(\Omega)} \le CH|\boldsymbol{u}|_{W^{1,4}(\Omega)}. \tag{42}$$

In addition, suppose that the solution p of (5)–(6) belongs to $W^{2,\frac{3}{2}}$; then

$$\|\bigtriangledown(p-p_H)\|_{L^{\frac{3}{2}}(\Omega)} \le Ch\left(|p|_{W^{2,\frac{3}{2}}} + |\boldsymbol{u}|_{W^{1,4}(\Omega)}\right) \tag{43}$$

with constant C independent of H.

To obtain the error estimates for the two-level algorithm, we start by rewriting (5)–(6) as follows: find $(\boldsymbol{u},p)\in X\times M$ such that

$$\begin{aligned}
&\frac{\mu}{\rho}\int_\Omega (K^{-1}\boldsymbol{u})\cdot\boldsymbol{\varphi}dx + \frac{\beta}{\rho}\int_\Omega |\boldsymbol{u_H}|_{\boldsymbol{\epsilon}}\boldsymbol{u}_H\cdot\boldsymbol{\varphi}d\boldsymbol{x} + \frac{\beta}{\rho}\int_\Omega \mathcal{D}\boldsymbol{f}_\epsilon(\boldsymbol{u}_H)(\boldsymbol{u}-\boldsymbol{u}_H)\cdot\boldsymbol{\varphi}d\boldsymbol{x}\\
&\quad + \int_\Omega \bigtriangledown p\cdot\boldsymbol{\varphi}d\boldsymbol{x} = \int_\Omega \boldsymbol{f}\boldsymbol{\varphi}dx - \frac{\beta}{\rho}\int_\Omega |\boldsymbol{u}|\boldsymbol{u}\cdot\boldsymbol{\varphi}d\boldsymbol{x} + \frac{\beta}{\rho}\int_\Omega |\boldsymbol{u_H}|_{\boldsymbol{\epsilon}}\boldsymbol{u}_H\cdot\boldsymbol{\varphi}d\boldsymbol{x}\\
&\quad + \frac{\beta}{\rho}\int_\Omega \mathcal{D}\boldsymbol{f}_\epsilon(\boldsymbol{u}_H)(\boldsymbol{u}-\boldsymbol{u}_H)\cdot\boldsymbol{\varphi}d\boldsymbol{x} \quad \forall\boldsymbol{\varphi}\in X,
\end{aligned} \tag{44}$$

$$\int_\Omega \bigtriangledown q\cdot\boldsymbol{u}d\boldsymbol{x} = -\int_\Omega bq\boldsymbol{d}x + \int_{\partial\Omega} gq\boldsymbol{d}\sigma \quad \forall q\in M\ . \tag{45}$$

In view of (18), (44)–(45) becomes

$$
\begin{aligned}
&\frac{\mu}{\rho}\int_\Omega (K^{-1}\boldsymbol{u})\cdot\boldsymbol{\varphi}dx + \frac{\beta}{\rho}\int_\Omega |\boldsymbol{u_H}|_{\boldsymbol{\epsilon}}\boldsymbol{u}_H\cdot\boldsymbol{\varphi}d\boldsymbol{x}\\
&\quad + \frac{\beta}{\rho}\int_\Omega \mathcal{D}\boldsymbol{f}_\epsilon(\boldsymbol{u}_H)(\boldsymbol{u}-\boldsymbol{u}_H)\cdot\boldsymbol{\varphi}d\boldsymbol{x} + \int_\Omega \bigtriangledown p\cdot\boldsymbol{\varphi}d\boldsymbol{x}\\
&= \int_\Omega \boldsymbol{f}\boldsymbol{\varphi}dx - \frac{\beta}{\rho}\int_\Omega |\boldsymbol{u}|\boldsymbol{u}\cdot\boldsymbol{\varphi}d\boldsymbol{x} + \frac{\beta}{\rho}\int_\Omega |\boldsymbol{u}|_{\boldsymbol{\epsilon}}\boldsymbol{u}\cdot\boldsymbol{\varphi}d\boldsymbol{x}\\
&\quad - \frac{\beta}{2!\rho}\int_\Omega \mathcal{D}^2\boldsymbol{f}_\epsilon(\boldsymbol{\zeta}_H)(\boldsymbol{u}-\boldsymbol{u}_H)^2\cdot\boldsymbol{\varphi}d\boldsymbol{x} \quad \forall\boldsymbol{\varphi}\in X\ ,
\end{aligned}
\tag{46}
$$

$$
\int_\Omega \bigtriangledown q\cdot\boldsymbol{u}d\boldsymbol{x} = -\int_\Omega bq\boldsymbol{d}x + \int_{\partial\Omega} gq\boldsymbol{d}\sigma \quad \forall q\in M\ . \tag{47}
$$

Furthermore, (23)–(24) can be rearranged as follows: for all $(\boldsymbol{\varphi_h}, q_h)\in X_h\times M_h$, find $(\boldsymbol{u}_h, p_h)\in X_h\times M_h$ such that

$$
\begin{aligned}
&\frac{\mu}{\rho}\int_\Omega (K^{-1}\boldsymbol{u}_h)\cdot\boldsymbol{\varphi}_h dx + \frac{\beta}{\rho}\int_\Omega |\boldsymbol{u_H}|_{\boldsymbol{\epsilon}}\boldsymbol{u_H}\cdot\boldsymbol{\varphi}_h d\boldsymbol{x} + \frac{\beta}{\rho}\int_\Omega \mathcal{D}\boldsymbol{f}_\epsilon(\boldsymbol{u}_H)(\boldsymbol{u}_h-\boldsymbol{u}_H)\cdot\boldsymbol{\varphi}_h d\boldsymbol{x}\\
&\qquad + \int_\Omega \bigtriangledown p_h\cdot\boldsymbol{\varphi}_h d\boldsymbol{x} = \int_\Omega \boldsymbol{f}\boldsymbol{\varphi}_h dx,
\end{aligned}
\tag{48}
$$

$$
\int_\Omega \bigtriangledown q_h\cdot\boldsymbol{u}_h d\boldsymbol{x} = -\int_\Omega bq_h\boldsymbol{d}x + \int_{\partial\Omega} gq_h\boldsymbol{d}\sigma. \tag{49}
$$

6.1. Error estimates for velocity. The error estimate for the velocity is given by the following proposition.

PROPOSITION 6.2. *Let* $(\boldsymbol{u_h}, p_h)$ *be the solution of* (23)–(24)*,* $(\boldsymbol{u_H}, p_H)$ *be the solution of* (21)–(22)*, and* $(\boldsymbol{u}, p)$ *be the solution of* (5)–(6) *and assume that* $(\boldsymbol{u}, p)\in L^3(\Omega)\times W^{1,2}(\Omega)$*. Then for any* $\boldsymbol{w_h}\in X_h$ *satisfying the constraint in* (24)*, the following error estimate holds:*

$$
\begin{aligned}
\|\boldsymbol{u}-\boldsymbol{u_h}\|_{L^2(\Omega)} \le &\left(1 + \frac{\|K^{-1}\|_{L^\infty(\Omega)}}{\lambda_{min}} + \frac{\beta}{\mu\lambda_{min}}(C_1+\epsilon)\right)\|\boldsymbol{u}-\boldsymbol{w_h}\|_{L^2(\Omega)}\\
&+ \frac{\beta C}{2!\mu\lambda_{min}}\|\boldsymbol{u}-\boldsymbol{u}_H\|^2_{L^2(\Omega)} + \frac{\rho}{\mu\lambda_{min}}\|\bigtriangledown(p-I_h(p))\|_{L^2(\Omega)}\\
&+ \frac{\beta}{\rho}\epsilon\|\boldsymbol{u}\|_{L^2(\Omega)}\ ,
\end{aligned}
\tag{50}
$$

where C *and* C_1 *are positive constants independent of* h *and* H*.*

Proof. Subtracting (48) from (46), we get

$$
\begin{aligned}
&\frac{\mu}{\rho}\int_\Omega K^{-1}(\boldsymbol{u}-\boldsymbol{u_h})\cdot\boldsymbol{\varphi_h}d\boldsymbol{x} + \frac{\beta}{\rho}\int_\Omega \mathcal{D}\boldsymbol{f}_\epsilon(\boldsymbol{u}_H)(\boldsymbol{u}-\boldsymbol{u}_h)\cdot\boldsymbol{\varphi}_h d\boldsymbol{x}\\
&\quad + \int_\Omega \bigtriangledown(p-p_h)\cdot\boldsymbol{\varphi}_h d\boldsymbol{x} = \frac{\beta}{2!\rho}\int_\Omega \mathcal{D}^2\boldsymbol{f}_\epsilon(\boldsymbol{\zeta}_H)\cdot(\boldsymbol{u}-\boldsymbol{u}_H)^2\cdot\boldsymbol{\varphi}_h d\boldsymbol{x}\\
&\quad + \frac{\beta}{\rho}\int_\Omega (|\boldsymbol{u}|_\epsilon - |\boldsymbol{u}|)\boldsymbol{u}\cdot\boldsymbol{\varphi}d\boldsymbol{x} \quad \forall\boldsymbol{\varphi}_h\in V_h.
\end{aligned}
\tag{51}
$$

Inserting $I_h(p)$ and using the fact that $\boldsymbol{\varphi}_h\in V_h$,

$$\begin{aligned}
&\frac{\mu}{\rho}\int_\Omega K^{-1}(\boldsymbol{u}-\boldsymbol{u_h})\cdot\boldsymbol{\varphi_h}d\boldsymbol{x}+\frac{\beta}{\rho}\int_\Omega \mathcal{D}\boldsymbol{f}_\epsilon(\boldsymbol{u}_H)(\boldsymbol{u}-\boldsymbol{u}_h)\cdot\boldsymbol{\varphi}_h d\boldsymbol{x}\\
&\quad=\frac{\beta}{2!\rho}\int_\Omega \mathcal{D}^2\boldsymbol{f}_\epsilon(\zeta_H)\cdot(\boldsymbol{u}-\boldsymbol{u}_H)^2\cdot\boldsymbol{\varphi}_h d\boldsymbol{x}+\int_\Omega \bigtriangledown(I_h(p)-p)\cdot\boldsymbol{\varphi_h}d\boldsymbol{x}\\
&\qquad+\frac{\beta}{\rho}\int_\Omega(|\boldsymbol{u}|_\epsilon-|\boldsymbol{u}|)\boldsymbol{u}\cdot\boldsymbol{\varphi}d\boldsymbol{x}\quad\forall\boldsymbol{\varphi_h}\in V_h\ .
\end{aligned}$$

Inserting $\boldsymbol{w_h}\in X_h$ yields

$$\begin{aligned}
&\frac{\mu}{\rho}\int_\Omega K^{-1}(\boldsymbol{u}_h-\boldsymbol{w}_h)\cdot\boldsymbol{\varphi_h}d\boldsymbol{x}+\frac{\beta}{\rho}\int_\Omega \mathcal{D}\boldsymbol{f}_\epsilon(\boldsymbol{u}_H)(\boldsymbol{u}_h-\boldsymbol{w}_h)\cdot\boldsymbol{\varphi}_h d\boldsymbol{x}\\
&\quad=\frac{\mu}{\rho}\int_\Omega K^{-1}(\boldsymbol{u}-\boldsymbol{w_h})\cdot\boldsymbol{\varphi_h}d\boldsymbol{x}+\frac{\beta}{\rho}\int_\Omega \mathcal{D}\boldsymbol{f}_\epsilon(\boldsymbol{u}_H)(\boldsymbol{u}-\boldsymbol{w}_h)\cdot\boldsymbol{\varphi}_h d\boldsymbol{x}\\
&\qquad-\frac{\beta}{\rho}\int_\Omega \mathcal{D}^2\boldsymbol{f}_\epsilon(\zeta_H)\cdot(\boldsymbol{u}-\boldsymbol{u}_H)^2\cdot\boldsymbol{\varphi}_h d\boldsymbol{x}+\int_\Omega \bigtriangledown(p-I_h(p))\cdot\boldsymbol{\varphi_h}d\boldsymbol{x}\\
&\qquad-\frac{\beta}{\rho}\int_\Omega(|\boldsymbol{u}|_\epsilon-|\boldsymbol{u}|)\boldsymbol{u}\cdot\boldsymbol{\varphi}_h d\boldsymbol{x}\quad\forall\boldsymbol{\varphi_h}\in V_h.
\end{aligned}\tag{52}$$

Choose $\boldsymbol{\varphi_h}=\boldsymbol{u_h}-\boldsymbol{w_h}$; then (52) can be written as

$$\tilde{T}=\sum_{i=1}^{5}T_i\tag{53}$$

with

$$\begin{aligned}
\tilde{T}&=\frac{\mu}{\rho}\int_\Omega K^{-1}(\boldsymbol{u_h}-\boldsymbol{w_h})\cdot(\boldsymbol{u}_h-\boldsymbol{w}_h)d\boldsymbol{x}\\
&\quad+\frac{\beta}{\rho}\int_\Omega \mathcal{D}\boldsymbol{f}_\epsilon(\boldsymbol{u_H})(\boldsymbol{u}_h-\boldsymbol{w}_h)\cdot(\boldsymbol{u}_h-\boldsymbol{w}_h)d\boldsymbol{x},
\end{aligned}\tag{54}$$

$$\begin{aligned}
T_1&=\frac{\mu}{\rho}\int_\Omega K^{-1}(\boldsymbol{u}-\boldsymbol{w}_h)\cdot(\boldsymbol{u}_h-\boldsymbol{w}_h)d\boldsymbol{x}\ ,\\
T_2&=\frac{\beta}{\rho}\int_\Omega \mathcal{D}\boldsymbol{f}_\epsilon(\boldsymbol{u}_H)(\boldsymbol{u}-\boldsymbol{w}_h)\cdot(\boldsymbol{u}_h-\boldsymbol{w}_h)d\boldsymbol{x}\ ,\\
T_3&=-\frac{\beta}{2!\rho}\int_\Omega \mathcal{D}^2\boldsymbol{f}_\epsilon(\zeta_H)\cdot(\boldsymbol{u}-\boldsymbol{u}_H)^2\cdot(\boldsymbol{u}_h-\boldsymbol{w}_h)d\boldsymbol{x}\ ,\\
T_4&=\int_\Omega \bigtriangledown(p-I_h(p))\cdot(\boldsymbol{u}_h-\boldsymbol{w}_h)d\boldsymbol{x}\ ,\\
T_5&=-\frac{\beta}{\rho}\int_\Omega(|\boldsymbol{u}|_\epsilon-|\boldsymbol{u}|)\boldsymbol{u}\cdot(\boldsymbol{u}_h-\boldsymbol{w}_h)d\boldsymbol{x}\ .
\end{aligned}\tag{55}$$

Thanks to Lemma 5.1, we estimate as follows:

$$\begin{aligned}
\left|\tilde{T}\right|&\geq\frac{\mu}{\rho}\lambda_{min}\|\boldsymbol{u}_h-\boldsymbol{w}_h\|^2_{L^2(\Omega)}+\frac{\beta}{\rho}\min_{i,j=1,2}\left|\frac{\partial\boldsymbol{f}_{\epsilon,i}(\boldsymbol{u}_H)}{\partial u_j}\right|\|\boldsymbol{u}_h-\boldsymbol{w}_h\|^2_{L^2(\Omega)}\\
&\geq\frac{\mu}{\rho}\lambda_{min}\|\boldsymbol{u}_h-\boldsymbol{w}_h\|^2_{L^2(\Omega)}\ ,
\end{aligned}\tag{56}$$

$$|T_1|\leq\frac{\mu}{\rho}\|K^{-1}\|_{L^\infty(\Omega)}\|\boldsymbol{u}-\boldsymbol{w_h}\|_{L^2(\Omega)}\|\boldsymbol{u_h}-\boldsymbol{w_h}\|_{L^2(\Omega)}\ ,$$

$$|T_2| \leq \frac{\beta}{\rho}\gamma\|\boldsymbol{u}-\boldsymbol{w_h}\|_{L^2(\Omega)}\|\boldsymbol{u_h}-\boldsymbol{w_h}\|_{L^2(\Omega)}, \quad \gamma = \max_i \sum_{j=1}^{2}\left|\frac{\partial \boldsymbol{f}_{\epsilon,i}(\boldsymbol{u}_H)}{\partial u_j}\right|$$

$$\leq \frac{\beta}{\rho}(C_1+\epsilon)\|\boldsymbol{u}-\boldsymbol{w_h}\|_{L^2(\Omega)}\|\boldsymbol{u_h}-\boldsymbol{w_h}\|_{L^2(\Omega)}, \text{ since (20) holds,}$$

$$|T_3| \leq \frac{\beta}{2!\rho}\int_\Omega \left|\sum_{k=1}^{2}\sum_{j=1}^{2}\sum_{i=1}^{2}\frac{\partial^2 \boldsymbol{f}_{\epsilon,k}(\boldsymbol{\zeta}_H)}{\partial u_i \partial u_j}(u_i-u_{H,i})(u_j-u_{H,j})(u_{h,k}-w_{h,k})\right| dx.$$

Using (20) and the facts $\|u_i - u_{H,i}\|_{L^2(\Omega)} \leq \|\boldsymbol{u}-\boldsymbol{u}_H\|_{L^2(\Omega)}$, $i = j = 1,2$, and $\|u_{h,k}-w_{h,k}\|_{L^2(\Omega)} \leq \|\boldsymbol{u}_h-\boldsymbol{w}_h\|_{L^2(\Omega)}$, $k=1,2$, we then arrive at

$$|T_3| \leq \frac{\beta}{2!\rho}C\|\boldsymbol{u}-\boldsymbol{u}_H\|^2_{L^2(\Omega)}\|\boldsymbol{u}_h-\boldsymbol{w}_h\|_{L^2(\Omega)}. \tag{57}$$

Furthermore,

$$|T_4| \leq \|\bigtriangledown(p-I_h(p))\|_{L^2(\Omega)}\|\boldsymbol{u_h}-\boldsymbol{w_h}\|_{L^2(\Omega)}\ , \tag{58}$$

$$|T_5| \leq \frac{\beta}{\rho}\epsilon\|\boldsymbol{u}\|_{L^2(\Omega)}\|\boldsymbol{u_h}-\boldsymbol{w_h}\|_{L^2(\Omega)}\ . \tag{59}$$

Substituting (56)–(59) in (53),

$$\begin{aligned}\frac{\mu}{\rho}\lambda_{min}\|\boldsymbol{u_h}-\boldsymbol{w_h}\|^2_{L^2(\Omega)} \leq\ & \frac{\mu}{\rho}\|K^{-1}\|_{L^\infty(\Omega)}\|\boldsymbol{u}-\boldsymbol{w_h}\|_{L^2(\Omega)}\|\boldsymbol{u_h}-\boldsymbol{w_h}\|_{L^2(\Omega)}\\ &+\frac{\beta}{\rho}(C_1+\epsilon)\|\boldsymbol{u}-\boldsymbol{w_h}\|_{L^2(\Omega)}\|\boldsymbol{u_h}-\boldsymbol{w_h}\|_{L^2(\Omega)}\\ &+\frac{\beta}{2!\rho}C\|\boldsymbol{u}-\boldsymbol{u}_H\|^2_{L^2(\Omega)}\|\boldsymbol{u}_h-\boldsymbol{w}_h\|_{L^2(\Omega)} \qquad (60)\\ &+\|\bigtriangledown(p-I_h(p))\|_{L^2(\Omega)}\|\boldsymbol{u_h}-\boldsymbol{w_h}\|_{L^2(\Omega)}\\ &+\frac{\beta}{\rho}\epsilon\|\boldsymbol{u}\|_{L^2(\Omega)}\|\boldsymbol{u_h}-\boldsymbol{w_h}\|_{L^2(\Omega)}\ . \qquad (61)\end{aligned}$$

Dividing through by $\frac{\mu}{\rho}\lambda_{min}\|\boldsymbol{u_h}-\boldsymbol{w_h}\|_{L^2(\Omega)}$ gives

$$\begin{aligned}\|\boldsymbol{u_h}-\boldsymbol{w_h}\|_{L^2(\Omega)} \leq\ & \frac{\|K^{-1}\|_{L^\infty(\Omega)}}{\lambda_{min}}\|\boldsymbol{u}-\boldsymbol{w_h}\|_{L^2(\Omega)}\\ &+\frac{\beta}{\mu\lambda_{min}}(C_1+\epsilon)\|\boldsymbol{u}-\boldsymbol{w_h}\|_{L^2(\Omega)}+\frac{\beta C}{2!\mu\lambda_{min}}\|\boldsymbol{u}-\boldsymbol{u}_H\|^2_{L^2(\Omega)}\\ &+\frac{\rho}{\mu\lambda_{min}}\|\bigtriangledown(p-I_h(p))\|_{L^2(\Omega)}+\frac{\beta}{\rho}\epsilon\|\boldsymbol{u}\|_{L^2(\Omega)}, \qquad (62)\end{aligned}$$

and (50) follows from (62). ∎

THEOREM 6.3. *Let $\mathcal{T}_h$ be a refinement of the triangulation $\mathcal{T}_H$ and satisfying* (14). *Take $\boldsymbol{w}_h = \Pi_h(\boldsymbol{u})$ as defined in* (38). *Then the approximate solution $\boldsymbol{u}_h$ satisfies the following order of convergence:*

$$\|\boldsymbol{u}-\boldsymbol{u_h}\|_{L^2(\Omega)} = O(\epsilon h + h + H^2 + \epsilon)\ . \tag{63}$$

Proof. It follows immediately from (50) by using the stability properties in (33) and the order of convergence in (42). ∎

Remark 6.4. For an appropriate choice of ϵ, (63) leads to a scaling $h = H^2$ between the coarse mesh size and fine mesh.

6.2. Error estimates for pressure. Furthermore, we obtain an error bound for the pressure in the next theorem.

THEOREM 6.5. *Suppose the assumptions of Theorem* 6.3 *hold. If the solution* p *of the problem* (5)–(6) *belongs to* $W^{2,\frac{3}{2}}(\Omega)$, *then there exists a constant* C *independent of* h *and* H *such that*

$$\left(\sum_{T\in\mathcal{T}_h} \| \triangledown (p-p_h)\|^{\frac{3}{2}}_{L^{3/2}(T)}\right)^{\frac{2}{3}} \leq C\left(\epsilon h + h + H^2 + \epsilon\right). \tag{64}$$

Proof. Subtracting (48) from (46), we get

$$\begin{aligned}\sum_{T\in\mathcal{T}_h}\int_T \triangledown(p-p_h)\cdot\boldsymbol{\varphi_h}d\boldsymbol{x} + \frac{\mu}{\rho}\int_\Omega K^{-1}(\boldsymbol{u}-\boldsymbol{u}_h)\cdot\boldsymbol{\varphi_h}d\boldsymbol{x} \\ + \frac{\beta}{\rho}\int_\Omega \mathcal{D}\boldsymbol{f}_\epsilon(\boldsymbol{u}_H)(\boldsymbol{u}-\boldsymbol{u}_h)\cdot\boldsymbol{\varphi_h}d\boldsymbol{x} \\ = \frac{\beta}{2!\rho}\int_\Omega \mathcal{D}^2\boldsymbol{f}_\epsilon(\boldsymbol{\zeta}_H)(\boldsymbol{u}-\boldsymbol{u}_H)^2d\boldsymbol{x} + \frac{\beta}{\rho}\int_\Omega(|\boldsymbol{u}|_\epsilon - |\boldsymbol{u}|)\boldsymbol{u}\cdot\boldsymbol{\varphi}_h d\boldsymbol{x} \quad \forall\boldsymbol{\varphi}_h\in X_h.\end{aligned} \tag{65}$$

Inserting $I_h(p)$ and rearranging we get

$$\begin{aligned}&\sum_{T\in\mathcal{T}_h}\int_T \triangledown(I_h(p)-p_h)\cdot\boldsymbol{\varphi_h}d\boldsymbol{x} \\ &\quad = -\frac{\mu}{\rho}\int_\Omega K^{-1}(\boldsymbol{u}-\boldsymbol{u}_h)\cdot\boldsymbol{\varphi_h}d\boldsymbol{x} - \frac{\beta}{\rho}\int_\Omega \mathcal{D}\boldsymbol{f}_\epsilon(\boldsymbol{u}_H)(\boldsymbol{u}-\boldsymbol{u}_h)\cdot\boldsymbol{\varphi_h}d\boldsymbol{x} \\ &\quad + \frac{\beta}{2!\rho}\int_\Omega \mathcal{D}^2\boldsymbol{f}_\epsilon(\boldsymbol{\zeta}_H)(\boldsymbol{u}-\boldsymbol{u}_H)^2\cdot\boldsymbol{\varphi_h}d\boldsymbol{x} + \frac{\beta}{\rho}\int_\Omega(|\boldsymbol{u}|_\epsilon - |\boldsymbol{u}|)\boldsymbol{u}\cdot\boldsymbol{\varphi}_h d\boldsymbol{x} \\ &\quad - \sum_{T\in\mathcal{T}_h}\int_T \triangledown(p-I_h(p))\cdot\boldsymbol{\varphi_h}d\boldsymbol{x} \quad \forall\boldsymbol{\varphi_h}\in X_h.\end{aligned} \tag{66}$$

It follows that

$$\begin{aligned}&\left|\sum_{T\in\mathcal{T}_h}\int_T \triangledown(I_h(p)-p_h)\cdot\boldsymbol{\varphi_h}d\boldsymbol{x}\right| \leq \frac{\mu}{\rho}\|K^{-1}\|_{L^\infty(\Omega)}|\Omega|^{\frac{1}{3}}\|\boldsymbol{u}-\boldsymbol{u}_h\|_{L^2(\Omega)}\|\boldsymbol{\varphi_h}\|_{L^3(\Omega)} \\ &\quad + \frac{\beta}{\rho}\max_i\sum_{j=1}^2\left|\frac{\partial\boldsymbol{f}_{\epsilon,i}(\boldsymbol{u}_H)}{\partial u_j}\right||\Omega|^{\frac{1}{3}}\|\boldsymbol{u}-\boldsymbol{u}_h\|_{L^2(\Omega)}\|\boldsymbol{\varphi_h}\|_{L^3(\Omega)} \\ &\quad + \frac{\beta}{2!\rho}\left|\sum_{k=1}^2\sum_{j=1}^2\sum_{i=1}^2\frac{\partial^2\boldsymbol{f}_{\epsilon,k}(\boldsymbol{\zeta}_H)}{\partial u_i\partial u_j}\right|\|(\boldsymbol{u}-\boldsymbol{u}_H)^2\|_{L^2(\Omega)}|\Omega|^{\frac{1}{3}}\|\boldsymbol{\varphi_h}\|_{L^3(\Omega)} \\ &\quad + \epsilon|\Omega|^{\frac{1}{3}}\|\boldsymbol{u}\|_{L^2(\Omega)}\|\boldsymbol{\varphi}_h\|_{L^3(\Omega)} + \|\triangledown(p-I_h(p))\|_{L^{\frac{3}{2}}(\Omega)}\|\boldsymbol{\varphi_h}\|_{L^3(\Omega)},\end{aligned}$$

and applying the bounds of the partial derivatives in Lemma 5.1 and dividing through by $\|\boldsymbol{\varphi_h}\|_{L^3(\Omega)}$,

$$\begin{aligned}&\left|\frac{1}{\|\boldsymbol{\varphi_h}\|_{L^3(\Omega)}}\sum_{T\in\mathcal{T}_h}\int_T \triangledown(I_h(p)-p_h)\cdot\boldsymbol{\varphi_h}d\boldsymbol{x}\right| \leq \frac{\mu}{\rho}\|K^{-1}\|_{L^\infty(\Omega)}|\Omega|^{\frac{1}{3}}\|\boldsymbol{u}-\boldsymbol{u}_h\|_{L^2(\Omega)} \\ &\quad + \frac{\beta}{\rho}(C_1+\epsilon)|\Omega|^{\frac{1}{3}}\|\boldsymbol{u}-\boldsymbol{u}_h\|_{L^2(\Omega)} + \frac{C\beta}{2!\rho}|\Omega|^{\frac{1}{3}}\|\boldsymbol{u}-\boldsymbol{u}_H\|^2_{L^2(\Omega)} + \epsilon|\Omega|^{\frac{1}{3}}\|\boldsymbol{u}\|_{L^2(\Omega)} \\ &\quad + \|\triangledown(p-I_h(p))\|_{L^{\frac{3}{2}}(\Omega)}.\end{aligned}$$

In view of the discrete infsup condition (28), we get

$$\left(\sum_{T\in\mathcal{T}_h}\|\nabla(I_h(p)-p_h)\|^{\frac{3}{2}}_{L^{3/2}(T)}\right)^{\frac{2}{3}} \le \left(\frac{\mu}{\rho}|\Omega|^{\frac{1}{3}}\|K^{-1}\|_{L^\infty(\Omega)}+\frac{\beta}{\rho}(C_1+\epsilon)|\Omega|^{\frac{1}{3}}\right)\|\boldsymbol{u}-\boldsymbol{u}_h\|_{L^2(\Omega)} + \frac{C\beta}{2!\rho}|\Omega|^{\frac{1}{3}}\|\boldsymbol{u}-\boldsymbol{u}_H\|^2_{L^2(\Omega)}+\epsilon|\Omega|^{\frac{1}{3}}\|\boldsymbol{u}\|_{L^2(\Omega)} + \|\nabla(p-I_h(p)\|_{L^{\frac{3}{2}}(\Omega)}\,. \tag{67}$$

Owing to the stability property of $I_h(p)$ in (41) and the error estimate in (50), we deduce (64). ∎

7. Linear and nonlinear systems of equations. In this section, we present the solutions of both the nonlinear system associated with the coarse mesh and the linear system associated with the fine mesh. As usual, we choose bases $X_H = span\{\boldsymbol{\varphi}_i\}_{i=1}^{n_1}$, $M_H = span\{\psi_i\}_{i=1}^{m_1}$, $X_h = span\{\boldsymbol{\Phi}_i\}_{i=1}^{n_2}$, and $M_h = span\{\Psi_i\}_{i=1}^{m_2}$. Then for any $\boldsymbol{u}_H\in X_H$, $p_H\in M_H$, and $\boldsymbol{u}_h\in X_h$, $p_h\in M_h$, can be expressed as

$$\boldsymbol{u}_H=\sum_{i=1}^{n_1}\tilde{u_1}^i\boldsymbol{\varphi}_i,\qquad p_H=\sum_{i=1}^{m_1}\tilde{p_1}^i\psi_i\ , \tag{68}$$

$$\tilde{u_1}=[\tilde{u_1}^1,\tilde{u_1}^2,\dots,\tilde{u_1}^{n_1}]^T,\quad \tilde{p_1}=[\tilde{p_1}^1,\tilde{p_1}^2,\dots,\tilde{p_1}^{m_1}]^T,$$

$$\boldsymbol{u}_h=\sum_{i=1}^{n_2}\tilde{u_2}^i\boldsymbol{\Phi}_i,\qquad p_h=\sum_{i=1}^{m_2}\tilde{p_2}^i\Psi_i\ , \tag{69}$$

$$\tilde{u_2}=[\tilde{u_2}^1,\tilde{u_2}^2,\dots,\tilde{u_2}^{n_2}]^T,\qquad \tilde{p_2}=[\tilde{p_2}^1,\tilde{p_2}^2,\dots,\tilde{p_2}^{m_2}]^T.$$

Now substituting (68) and (69) into (21)–(22), (23)–(24), respectively, results in the systems of equation given below. Find $\tilde{u}_1\in\mathbb{R}^{n_1}$, $\tilde{p}_1\in\mathbb{R}^{m_1}$ such that

$$\begin{bmatrix} D(\tilde{u}_1) & B^T\\ B & 0\end{bmatrix}\begin{bmatrix}\tilde{u}_1\\ \tilde{p}_1\end{bmatrix}=\begin{bmatrix}G_1\\ G_2\end{bmatrix}. \tag{70}$$

Find $\tilde{u}_2\in\mathbb{R}^{n_2}$, $\tilde{p}_2\in\mathbb{R}^{m_2}$ such that

$$\begin{bmatrix} \bar{D}(\tilde{u}_1) & \bar{B}^T\\ \bar{B} & 0\end{bmatrix}\begin{bmatrix}\tilde{u}_2\\ \tilde{p}_2\end{bmatrix}=\begin{bmatrix}\bar{G}_1\\ \bar{G}_2\end{bmatrix}. \tag{71}$$

$D(\tilde{u}_1)\in\mathbb{R}^{n_1\times n_1}$ is a diagonal matrix and $D(\tilde{u}_1)\tilde{u}_1$ is a nonlinear vector function corresponding to

$$\frac{\mu}{\rho}\int_\Omega K^{-1}\boldsymbol{u}_H\cdot\boldsymbol{\varphi}_H d\boldsymbol{x}+\frac{\beta}{\rho}\int_\Omega|\boldsymbol{u}_H|\boldsymbol{u}_H\cdot\boldsymbol{\varphi}_H d\boldsymbol{x}\ .$$

$\bar{D}(\tilde{u}_1)\in\mathbb{R}^{n_2\times n_2}$ is a diagonal matrix and $\bar{D}(\tilde{u}_1)\tilde{u}_2$ is a linear vector function corresponding to

$$\frac{\mu}{\rho}\int_\Omega(K^{-1}\boldsymbol{u}_h)\cdot\boldsymbol{\varphi}_h dx+\frac{\beta}{\rho}\int_\Omega\mathcal{D}\boldsymbol{f}_\epsilon(\boldsymbol{u}_H)\boldsymbol{u}_h\cdot\boldsymbol{\varphi}_h d\boldsymbol{x}.$$

$B\in\mathbb{R}^{m_1\times n_1}$, $B^T\in\mathbb{R}^{n_1\times m_1}$ are matrices corresponding to

$$\int_\Omega\nabla q_H\cdot\boldsymbol{u}_H d\boldsymbol{x},\quad \int_\Omega\nabla p_H\cdot\boldsymbol{\varphi}_H d\boldsymbol{x}\ ,$$

respectively. $\bar{B} \in \mathbb{R}^{m_2 \times n_2}$, $\bar{B}^T \in \mathbb{R}^{n_2 \times m_2}$ are matrices corresponding to

$$\int_\Omega \nabla q_h \cdot \boldsymbol{u}_h d\boldsymbol{x}, \quad \int_\Omega \nabla p_h \cdot \boldsymbol{\varphi}_h d\boldsymbol{x} \ ,$$

respectively, $\boldsymbol{G}_1$ and $\boldsymbol{G}_2$ are vectors corresponding to

$$\int_\Omega \boldsymbol{f} \cdot \boldsymbol{\varphi}_H dx, \quad -\int_\Omega b q_H \boldsymbol{d}x + \int_{\partial\Omega} g q_H \boldsymbol{d}\sigma \ ,$$

respectively, $\bar{\boldsymbol{G}}_1$ and $\bar{\boldsymbol{G}}_2$ are vectors corresponding to

$$\int_\Omega \boldsymbol{f} \boldsymbol{\varphi}_h dx - \frac{\beta}{\rho} \int_\Omega |\boldsymbol{u_H}|_{\boldsymbol{\epsilon}} \boldsymbol{u_H} \cdot \boldsymbol{\varphi}_h d\boldsymbol{x} + \frac{\beta}{\rho} \int_\Omega \mathcal{D} \boldsymbol{f}_\epsilon(\boldsymbol{u}_H) \boldsymbol{u}_H \cdot \boldsymbol{\varphi}_h d\boldsymbol{x},$$
$$-\int_\Omega b q_h \boldsymbol{d}x + \int_{\partial\Omega} g q_h \boldsymbol{d}\sigma \ ,$$

respectively.

8. Numerical results. In this section, we present some numerical results to validate the effectiveness of the two-level algorithm. The purpose of this section is first to illustrate the computational efficiency of the two-level method and second to verify the theoretical rates of convergence developed in section 6. The nonlinear system (70) on the coarse mesh is solved by Newton's method [22, 29] until the norm of the difference in successive iterates and the norm of residual are within a fixed tolerance of $1e-6$. The linear system (71) on the fine mesh has a saddle point structure [4], and it is solved using MINRES [30]. In this section, we consider two test problems.

8.1. Problem with known solution. In this subsection, we consider an example taken from [37, 38].

Example 8.1. Consider

$$\Omega = \left\{(x, y) \in \mathbb{R}^2, -1 < x < 1, -1 < y < 1\right\} \ ,$$

$$\boldsymbol{f(x,y)} = \begin{bmatrix} 2y(1-x^2)\left(1 + 2\beta\sqrt{y^2(1-x^2)^2 + x^2(1-y^2)^2}\right) + 3x^2 \\ -2x(1-y^2)\left(1 + 2\beta\sqrt{y^2(1-x^2)^2 + x^2(1-y^2)^2}\right) + 3y^2 \end{bmatrix}$$

and $g(x, y) = 0$ on $\partial\Omega$. Then the exact velocity and pressure are given as follows:

$$\boldsymbol{u}(x, y) = \left(2y(1-x^2), -2x(1-y^2)\right)^T, \quad p(x, y) = x^3 + y^3.$$

8.1.1. Computational efficiency. Here we compare the simulation time for the standard one-level method (i.e., the full nonlinear system, without the two-level method) with the simulation time for the two-level method. For this experiment, K is assumed to be I_{2X2}, and μ and ρ are taken to be 1. The non-Darcy parameter β is assumed to be 10, $\epsilon = 10^{-3}$. In Tables 1 and 2, the degrees of freedom of the velocity field and pressure are tabulated, showing the division of huge nonlinear systems of equations into a smaller nonlinear system of the equations on the coarse mesh followed by a large linear system on the fine mesh. Figure 1 shows the computed two-level method solution.

The simulation time for different mesh sizes for both one-level and two-level methods for Example 8.1 are presented in Tables 3 and 4, respectively. The two-level method appears to be much cheaper than the one-level method for smaller values of h without compromising accuracy.

Table 1
Degrees of freedom of one-level method.

h	DoFu_h	DoFp_h	DoF fine
1/16	1024	289	1313
1/36	5184	1369	6553
1/100	40000	10201	50201
1/144	82944	21025	103969

Table 2
Degrees of freedom of two-level method.

H	h	DoFu_H	DoFp_H	DoFu_h	DoFp_h	DoF coarse	DoF fine
1/4	1/16	64	25	1024	289	89	1313
1/6	1/36	144	49	5184	1369	193	6553
1/10	1/100	400	121	40000	10201	521	50201
1/12	1/144	576	169	82944	21025	745	103969

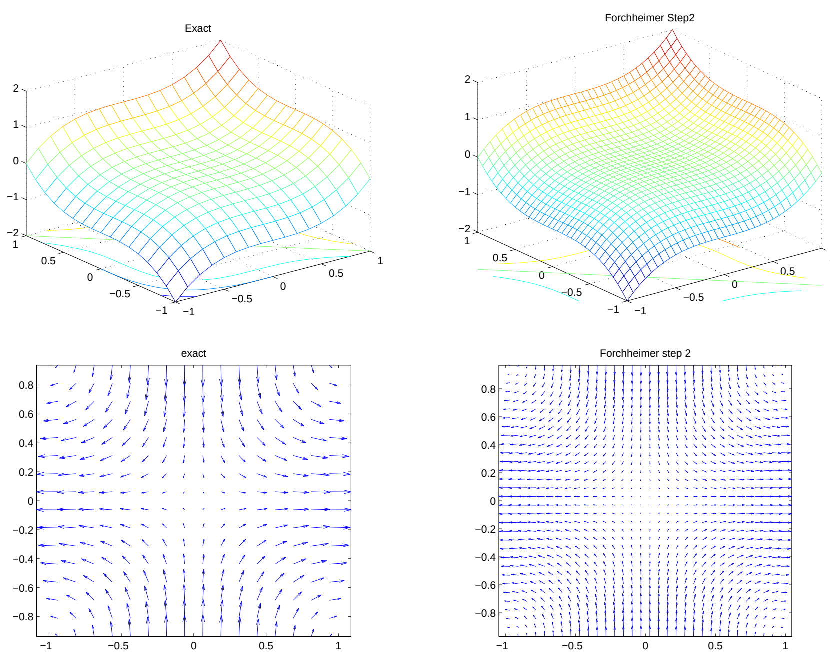

Fig. 1. *Pressure and velocity profiles for Example* 8.1. *Left: Exact pressure and velocity field. Right: Two-level pressure and velocity field.*

8.1.2. Rate of convergence. The L^2-errors of the velocity and its rate of convergence for one-level and two-level methods are presented in Tables 5 and 6, respectively. From Figure 2, we can observe that the two-level and one-level approximations velocities have first-order accuracy in the L^2-norm. The rates of convergence agree with the result in (50).

8.2. Five-spot problem. In this subsection, we consider the five-spot problem, which is a well known test problem for numerical techniques in reservoir simulation.

TABLE 3
CPU time for one-level MFEM method for Example 8.1.

h	$\|\boldsymbol{u}-\boldsymbol{u}_h\|_{L^2(\Omega)}$	CPU (sec.)
1/16	0.20263	2.31759
1/36	0.09346	2.2955
1/64	0.05645	62.4759
1/100	0.04078	266.195
1/144	0.03334	1005.27

TABLE 4
CPU time for two-level MFEM method for Example 8.1.

H	h	$\|\boldsymbol{u}-\boldsymbol{u}_h\|_{L^2(\Omega)}$	CPU (sec.)
1/4	1/16	0.20095	2.29551
1/6	1/36	0.09061	2.66802
1/8	1/64	0.05182	8.98689
1/10	1/100	0.03416	28.0365
1/12	1/144	0.02489	78.2143

TABLE 5
Error and order of convergence for one-level method for Example 8.1.

h	$\|\boldsymbol{u}-\boldsymbol{u}_{\boldsymbol{h}}\|_{L^2(\Omega)}$	L^2-order
1/8	0.3901	—
1/16	0.20263	0.9450
1/32	0.10151	0.9972
1/64	0.0522	0.9595
1/128	0.02738	0.9309

TABLE 6
Error and order of convergence for two-level method for Example 8.1.

H	h	$\|\boldsymbol{u}-\boldsymbol{u}_{\boldsymbol{h}}\|_{L^2(\Omega)}$	L^2-order
1/4	1/8	0.39134	—
1/8	1/16	0.20075	0.96302
1/16	1/32	0.10157	0.98301
1/32	1/64	0.05167	0.97481
1/64	1/128	0.02734	0.91839

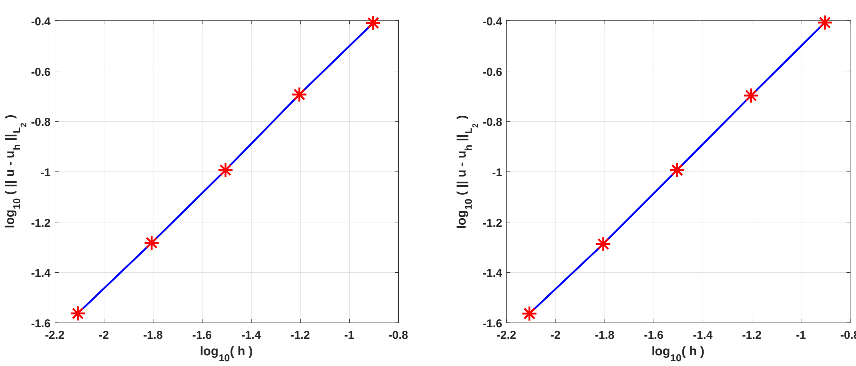

FIG. 2. *log-log plot of velocity errors. Left: One-level MFEM. Right: Two-level MFEM.*

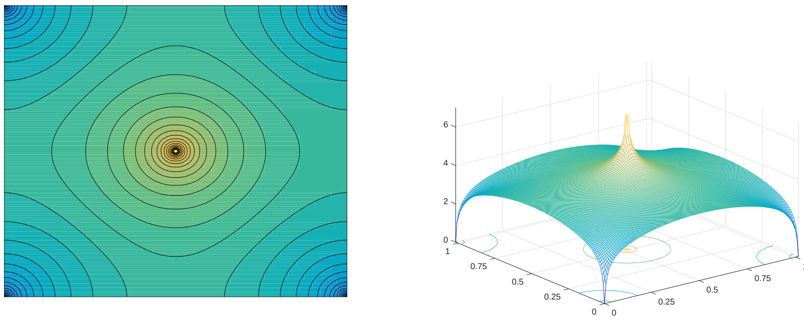

FIG. 3. *Pressure profile for the five-spot problem. Left: Pressure streamlines. Right: Three-dimensional pressure surface.*

Example 8.2. We consider an isotropic and homogeneous permeability $K = 1$ for all $x \in \Omega = [-1, 1] \times [-1, 1]$. We place one injection well at the center and four production wells at the corners and no-flow conditions at the boundaries [1].

The pressure profile of Example 8.2 is shown in Figure 3. The profile is as expected of a five-spot problem, and high pressure distributions are observed at the corners of the square (production wells).

9. Conclusion. In this paper, we formulated and implemented a two-level mixed finite algorithm for the nonlinear Darcy–Forchheimer equation modeling a single-phase steady non-Darcy flow porous media. In order to construct the two-level algorithm, the nonlinear term was modified to allow up to second-order Taylor series expansion. Numerical experiments for the two-level algorithm with piecewise constant velocities and continuous piecewise linear pressures were carried out. The numerical results verified the theoretical error estimates, with respect to both the coarse mesh size, H, and the fine mesh size, h. We proved that the error estimates of the two-level mixed finite element algorithm are of order $\mathrm{O}(\epsilon h + h + H^2 + \epsilon)$ for velocity and pressure. Furthermore, the two-level method significantly decreases the computational time of the standard one-level method while maintaining accuracy. The two-level method also proved to provide a good solution for highly nonlinear flows.

Acknowledgments. The authors are grateful to the King Fahd University of Petroleum and Minerals for providing support.

REFERENCES

[1] J. Aarnes, T. Gimse, and K. Lie, *An introduction to the numerics of flow in porous media using MATLAB*, in Geometrical Modeling, Numerical Simulation and Optimisation, Industrial Mathematics at SINTEF, G. Hasle, K. Lie, and E. Quak, eds., Springer, Berlin, 2007, pp. 265–306.

[2] R. A. Adams, *Sobolev Spaces*, Academic Press, New York, 1975.

[3] I. Babuška, *The finite element method with Lagrangian multipliers*, Numer. Math., 20 (1973), pp. 179–192.

[4] M. Benzi, G. H. Golub, and J. Liesen, *Numerical solution of saddle point problems*, Acta Numer., 14 (2005), pp. 1–137.

[5] D. Boffi, F. Brezzi, and M. Fortin, *Mixed Finite Element Methods and Applications*, Springer Ser. Comput. Math. 44, Springer, Berlin, 2013.

[6] F. Brezzi, *On the existence, uniqueness and approximation of saddle-point problems arising from Lagrangian multipliers*, RAIRO Anal. Numer., 8 (1974), pp. 129–151.

[7] Y. Chen, H. Liu, and S. Liu, *Analysis of two-grid methods for reaction-diffusion equations by expanded mixed finite element methods*, Internat. J. Numer. Methods Engrg., 69 (2007), pp. 408–422.
[8] P. G. Ciarlet, *The Finite Element Method for Elliptic Problems*, North-Holland, Amsterdam, 1978.
[9] C. N. Dawson and M. F. Wheeler, *Two-grid methods for mixed finite element approximations of nonlinear parabolic equation*, Contemp. Math., 180 (1994), pp. 191–203.
[10] C. N. Dawson, M. F. Wheeler, and C. S. Woodward, *A two-grid finite difference scheme for nonlinear parabolic equations*, SIAM J. Numer. Anal., 35 (1998), pp. 435–452.
[11] F. Fairag, *A two-level finite-element discretization of the stream function form of the Navier-Stokes equations*, Comput. Math. Appl., 36 (1998), pp. 117–127.
[12] F. Fairag, *Two level finite element technique for pressure recovery from stream function formulation of the Navier-Stokes equations*, in Multiscale and Multiresolution Methods, T. J. Barth, T. Chan, and R. Haimes, eds., Springer, Berlin, 2002, pp. 297–306.
[13] F. Fairag, *Numerical computations of viscous, incompressible flow problems using a two-level finite element method*, SIAM J. Sci. Comput., 24 (2003), pp. 1919–1929.
[14] E. L. Foster, T. Iliescu, and D. R. Wells, *A two-level finite element discretization of the streamfunction formulation of the stationary quasi-geostrophic equations of the ocean*, Comput. Math. Appl., 66 (2013), pp. 1261–1271.
[15] V. Girault and P. Raviart, *Finite Element Approximation of the Navier-Stokes Equations*, Springer-Verlag, Berlin, 1986.
[16] V. Girault and M. F. Wheeler, *Numerical discretization of a Darcy-Forchheimer model*, Numer. Math., 110 (2008), pp. 161–198.
[17] Y. He, *Two-level method based on finite element and Crank-Nicolson extrapolation for the time-dependent Navier-Stokes equations*, SIAM J. Numer. Anal., 41 (2003), pp. 1263–1285.
[18] Y. He, *A two-level finite element Galerkin method for the nonstationary Navier-Stokes equations* I: *Spatial discretization*, J. Comput. Math., (2004), pp. 21–32.
[19] Y. He and K. Li, *Two-level stabilized finite element methods for the steady Navier-Stokes problem*, Computing, 74 (2005), pp. 337–351.
[20] J. S. Howell and N. J. Walkington, *Inf-sup conditions for twofold saddle point problems*, Numer. Math., 118 (2011), pp. 663–693.
[21] J. Huang, L. Chen, and H. Rui, *Multigrid methods for a mixed finite element method of the Darcy-Forchheimer model*, J. Sci. Comput., (2016), pp. 1–16.
[22] C. T. Kelley, *Solving Nonlinear Equations with Newton's Method*, Fundam. Algorithms 1, SIAM, Philadelphia, 2003.
[23] W. Layton, *A two-level discretization method for the Navier-Stokes equations*, Comput. Math. Appl., 26 (1993), pp. 33–38.
[24] W. Layton and H. Lenferink, *A multilevel mesh independence principle for the Navier-Stokes equations*, SIAM J. Numer. Anal., 33 (1996), pp. 17–30.
[25] W. Layton and W. Lenferink, *Two-level Picard and modified Picard methods for the Navier-Stokes equations*, Appl. Math. Comput., 69 (1995), pp. 263–274.
[26] W. Layton and L. Tobiska, *A two-level method with backtracking for the Navier-Stokes equations*, SIAM J. Numer. Anal., 35 (1998), pp. 2035–2054.
[27] X. Li and H. Rui, *A two-grid block-centered finite difference method for nonlinear non-Fickian flow model*, Appl. Math. Comput., 281 (2016), pp. 300–313.
[28] H. López, B. Molina, and J. J. Salas, *Comparison between different numerical discretizations for a Darcy-Forchheimer model*, Electron. Trans. Numer. Anal., 34 (2009), pp. 187–203.
[29] J. M. Ortega and W. C. Rheinboldt, *Iterative Solution of Nonlinear Equations in Several Variables*, Classics in Appl. Math. 30, SIAM, Philadelphia, 2000.
[30] C. C. Paige and M. A. Saunders, *Solution of sparse indefinite systems of linear equations*, SIAM J. Numer. Anal., 12 (1975), pp. 617–629.
[31] H. Pan and H. Rui, *Mixed element method for two-dimensional Darcy-Forchheimer model*, J. Sci. Comput., 52 (2012), pp. 563–587.
[32] E. J. Park, *Mixed finite element methods for generalized Forchheimer flow in porous media*, Numer. Methods Partial Differential Equations, 21 (2005), pp. 213–228.
[33] H. Rui and W. Liu, *A two-grid block-centered finite difference method for Darcy-Forchheimer flow in porous media*, SIAM J. Numer. Anal., 53 (2015), pp. 1941–1962.
[34] H. Rui and H. Pan, *A block-centered finite difference method for the Darcy-Forchheimer model*, SIAM J. Numer. Anal., 5 (2012), pp. 2612–2631.
[35] H. Rui and H. Pan, *A block-centered finite difference method for slightly compressible Darcy–Forchheimer flow in porous media*, J. Sci. Comput., 73 (2017), pp. 70–92.

[36] H. Rui, D. Zhao, and H. Pan, *A block-centered finite difference method for Darcy-Forchheimer model with variable Forchheimer number*, Numer. Methods Partial Differential Equations, 31 (2015), pp. 1603–1622.

[37] J. J. Salas, H. López, and B. Molina, *An analysis of a mixed finite element method for a Darcy-Forchheimer model*, Math. Comput. Model., 57 (2013), pp. 2325–2338.

[38] J. M. Urquiza, D. N'Dri, A. Garon, and M. Delfour, *A numerical study of primal mixed finite element approximations of Darcy equations*, Commun. Numer. Methods Engrg., 22 (2006), pp. 901–915.

[39] Y. Wang and H. Rui, *Stabilized Crouzeix-Raviart element for Darcy-Forchheimer model*, Numer. Methods Partial Differential Equations, 31 (2015), pp. 1568–1588.

[40] J. Xu, *A novel two-grid method for semilinear elliptic equations*, SIAM J. Sci. Comput., 15 (1994), pp. 231–237.

[41] J. Xu, *Two-grid discretization techniques for linear and nonlinear PDEs*, SIAM J. Numer. Anal., 33 (1996), pp. 1759–1777.